Biotechnology Reports 15 (2017) 33–40

Contents lists available at ScienceDirect

Biotechnology Reports

journal homepage: www.elsevier.com/locate/btre

Synthesis of silver nanoparticles using bacterial exopolysaccharide and its application for degradation of azo-dyes

Chinnashanmugam Saravanan[a], Rajendiran Rajesh[b], Thanamegam Kaviarasan[c], Krishnan Muthukumar[c], Digambar Kavitake[a], Prathapkumar Halady Shetty[a,*]

[a] Department of Food Science and Technology, Pondicherry University, Pondicherry 605014, India
[b] Department of Chemistry, Pondicherry University, Pondicherry 605014, India
[c] Department of Marine Science, Bharathidasan University 620024, India

ARTICLE INFO

Article history:
Received 11 September 2016
Received in revised form 21 February 2017
Accepted 27 February 2017
Available online 13 June 2017

Keywords:
Exopolysaccharide
AgNPs
characterization
azo dyes degradation
SEM-TEM

ABSTRACT

In this study, the synthesis and characterization of exopolysaccharide-stabilized sliver nanoparticles (AgNPs) was carried out for the degradation of industrial textile dyes. Characterization of AgNPs was done using surface plasmon spectra using UV–Vis spectroscopy, X-ray diffraction (XRD) and Raman spectroscopy. The morphological nature of AgNPs was determined through transmission electron microscopy (TEM), scanning electron microscopy (SEM) and atomic force microscopy (AFM), which indicated that the AgNPs were spherical in shape, with an average size of 35 nm. The thermal behaviour of AgNPs revealed that it is stable up to 437.1 °C and the required energy is 808.2J/g in TGA-DTA analysis. Ability of EPS stabilized AgNPs for degradation of azo dyes such as Methyl orange (MO) and Congo red (CR) showed that EPS stabilized AgNPs were found to be efficient in facilitating the degradation process of industrial textile dyes. The electron transfer takes place from reducing agent to dye molecule via nanoparticles, resulting in the destruction of the dye chromophore structure. This makes EPS-AgNPs a suitable, cheap and environment friendly candidate for biodegradation of harmful textile dyes.

1. Introduction

Synthesis of diverse nano-materials are the keystone of nanotechnology for its application in different fields such as medicines (drug delivery, drug targeting, cell imaging and biosensors), food sciences (nano-composites, nano-emulsions, nano-encapsulation etc.) and environmental sciences (bio-flocculant, microbial monitoring and detection, and chemical degradation [1,2]. Food-grade micro-particles and nanoparticles are synthesized from different range of ingredients such as biopolymers, surfactants, minerals and lipids and they own the ability to alter the functional behaviour of foods that is they can make the foods suitable for human health [4]. Many microflora can produce nanoparticles through both intra and extracellular levels. Silver nanoparticles (AgNPs) are used as a nanomaterial most commonly in various consumer products [3]. Synthesis of AgNPs can be performed in various parts of the microbial cells [5]. The purified polysaccharides from plants, animals and microflora sources were used as reducing and stabilizing agents for the synthesis of nanoparticles [6,7]. Polysaccharides have hydroxyl and hemiacetal groups, which plays a vital role in reduction and stabilization that generate vast chances for their application and probable mass production. It increases the eco-friendly approach characteristics of nanoparticles to avoid using toxic chemicals in the demand of growing technological processes [8]. Several lactic acid bacteria (LAB) such as *Lactobacillus spp.*, *Pediococcus pentosaceus* and *Enterococcus faecium* are able to reduce silver ions to silver nanoparticles. LAB produces diverse categories of exopolysaccharides containing different monomers (glucose, galactose, mannose and fructose) those are known to involve in redox reaction to synthesize silver nanoparticles (AgNPs) [10]. Recently, it was found that the AgNPs with a high surface area have more reactivity towards chemicals compounds and are effective tools in treatment of waste water within a short time period [11]. Chitosan-stabilized AgNPs combined with advanced oxidation process (AOP) showed good results in the degradation of various dyes [12].

Recently, AgNPs are extensively used to degrade the organic dyes through redox potential techniques and photocatalytic reaction under solar radiation [13,14]. In this study, we characterized the exopolysaccharide stabilized AgNPs for degradation of Methyl orange (MO) and Congo red (CR).

* Corresponding author.
E-mail address: pkshalady@yahoo.co.uk (P.H. Shetty).

http://dx.doi.org/10.1016/j.btre.2017.02.006

2. Materials and Methods

2.1. Bacterial strain and chemicals

The EPS producing strain *Leuconostoc lactis* was isolated from idli batter (an acidic fermented food) and has been characterized through 16 s rRNA level (NCBI Gene bank submission ID KC117496) which further used as the source of exopolysaccharide in this work [15]. All reagents used were of analytical grade.

2.2. Growth condition for L. lactis KC117496

For preparation of inoculum, a loopful of *L. lactis* was transferred into 5 mL MRS medium supplemented with 2% sucrose. For EPS production, 10 mL of culture was used as an inoculum in 100 mL of MRS broth (2% sucrose) and incubated under shaking conditions (rpm) for 48 h at 30 °C [15].

2.3. Extraction and purification of EPS

The fermented broth was harvested after 48 h and the cell suspension was heated to 100 °C for 10 min to inactivate the enzymes. Further, the suspension was cooled to room temperature and centrifuged at 4100 x g for 20 min to remove the biomass. The crude solution was further treated with Sevage reagent (chloroform: n-butanol at 5:1 v/v) three times to remove the proteinaceous materials. EPS was precipitated with cold ethanol (thrice volume) and left overnight at 4 °C. The precipitate was collected through centrifugation at 19200 x g for 15 min and dissolved in Milli Q water. Afterwards, it was encased in a dialysis bag (12–14 KDa) and dialyzed at 4 °C with Milli Q water for 48 h for partial purification. The sugar content of EPS was analysed using phenol sulphuric acid method [16]. The EPS was characterized by using FT-IR, HPTLC, NMR, AFM, SEM, TGA and XRD analysis which revealed the presence of only glucose monomers, indicating the glucan nature of EPS consisting α-(1→6) and α-(1→3) glycosidic linkages [15].

2.4. Synthesis of polymeric silver nanoparticles (EPS-AgNPs)

The partially purified EPS (10 mg) was dissolved in 10 mL of Milli Q water to form a uniform dispersion and 9 mM $AgNO_3$ was added under stirring condition. Subsequently, this solution was stored in a dark place at room temperature. After 24 h, the colourless solution changed to yellow, indicating the formation of polymeric sliver nanoparticles. Furthermore, to increase the concentration of solution it was further kept under incubation for 1 month. Samples were taken at various intervals and in between to know the progress of nanoparticle formation. Afterwards, the solution was centrifuged at 19200 x g for 15 min. The pellet was collected and air dried at room temperature for further analysis [17].

2.5. Characterization of sliver nanoparticles

2.5.1. UV–vis Spectroscopy

The reduction of Ag^+ ions with EPS to form sliver nanoparticles was observed after 1, 5, 10, 20 and 30 days of incubation under UV–Vis spectroscopy (UV-1800, Shimadzu) in the range of 300 to 800 nm [17].

2.5.2. TEM and SEM analysis

A drop of EPS-AgNPs was distributed onto a carbon copper grid and dried completely using a vacuum desiccator. The images were obtained using a transmission electron microscope (TEM) and a scanning electron microscope (SEM-Hitachi, Model: S-3400N) [18].

2.5.3. AFM analysis

About 5–10 μL of EPS-AgNPs was distributed on a mica disc (Pelco mica disc 10 mm) by a spin rotating plate and absolute ethanol was dropped over the sample to fix it on the mica disc. Then, the mica sheet was air-dried to remove the residual ethanol. The AFM images were captured using a scanning probe microscope (Brukers MM8) in tapping mode. The cantilever oscillated at its appropriate frequency (158 kHz) and ambitious amplitude (0.430 V) [19].

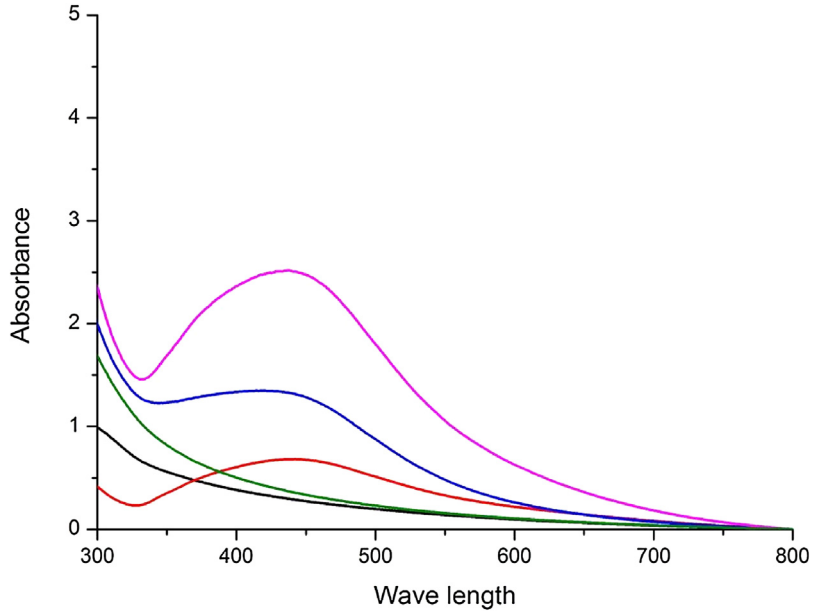

Fig. 1. Uv-Vis spectroscopy indicating the synthesis of EPS-AgNPs in increasing order during different storage period (Black–0 h, Green- 1 day, Red-10 days, Blue-20 days, Violet-30 days).

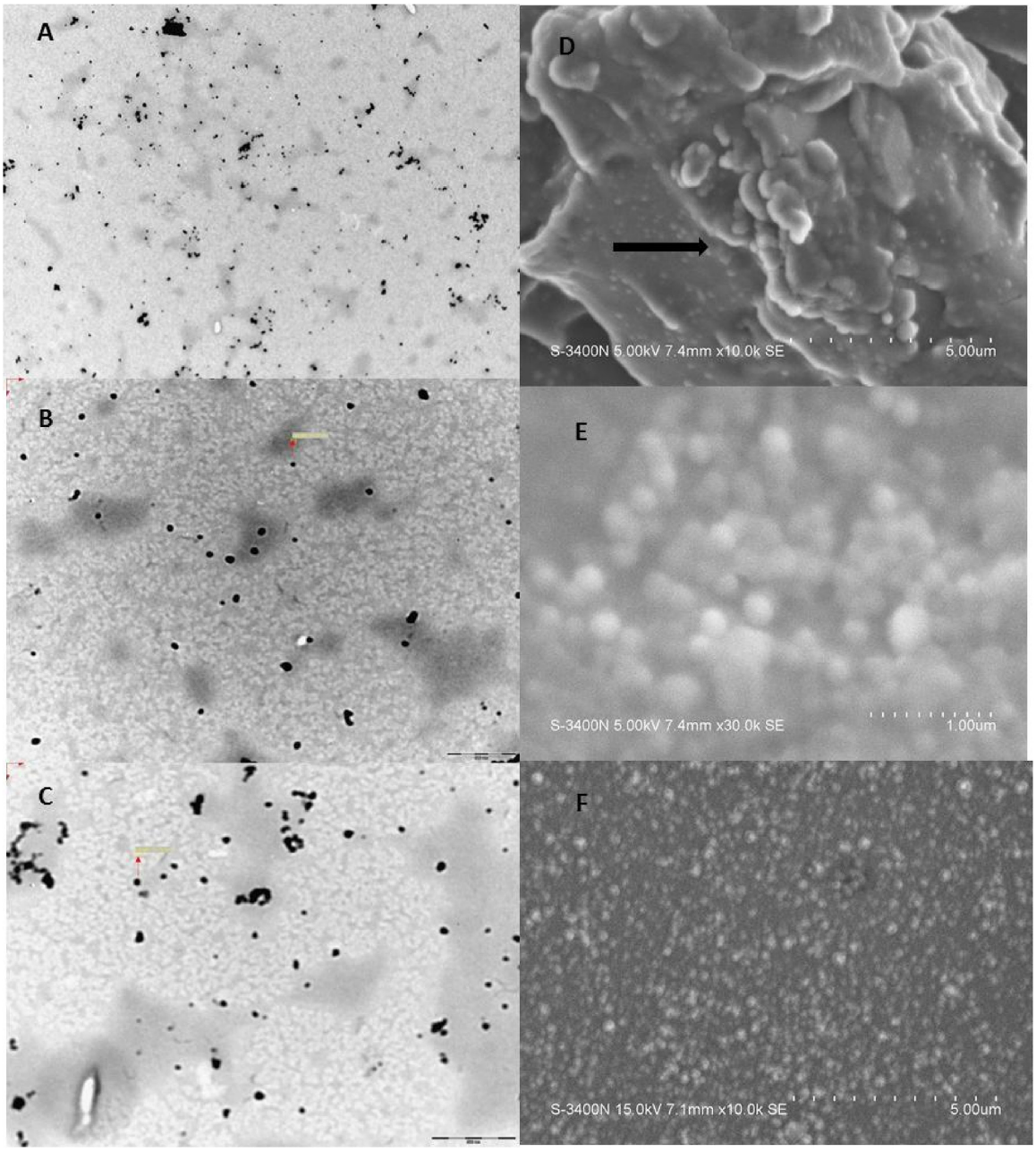

Fig. 2. TEM and SEM analysis of EPS stabilized AgNPs.
A, B and C TEM images indicated the size and dispersion of nanoparticles at various magnifications. D image showed the synthesis of AgNPs from the EPS. E and F exhibit the morphology of EPS stabilized AgNPs from SEM.

2.5.4. XRD and TGA-DTA analysis

To detect the EPS-AgNPs, a scan was performed within the two-theta angle range (20 and 80 °C) in X-ray diffraction (XRD). The polymeric nanoparticles were grounded to make fine powder and mounted on a quartz substrate and intensity peaks were recorded continuously using X-ray powder diffractometer (Philips X'pert pro, the Netherlands) with a Cu Tube X-ray produced at 40 kV and 30 mA with PW3011/20 proportional detector [15,18]. TG-DTA analysis of EPS-AgNPs was carried out in a thermal system (TG-DTA/DSC Model: Q600 SDT). About 10 mg of dried sample was used for the TG-DTA experiment. TG-DTA thermograms were obtained in the range of 0–400 °C under the flow of nitrogen air at the rate of 10 °C min^{-1}. Their distinct graphs were plotted with weight (percentage) loss and heat flow against temperature [20].

2.5.5. Raman Spectroscopy

The EPS-AgNPs powder was kept above the slide and the Raman spectra was recorded in the range 400–4000 cm^{-1} in 515 nm argon ion laser [21].

2.6. Degradation of organic azo-dyes in aqueous solution by EPS-AgNPs

The catalytic degradation of organic azo-dyes such as methyl orange (MO) and Congo red (CR) were monitored using UV–Vis

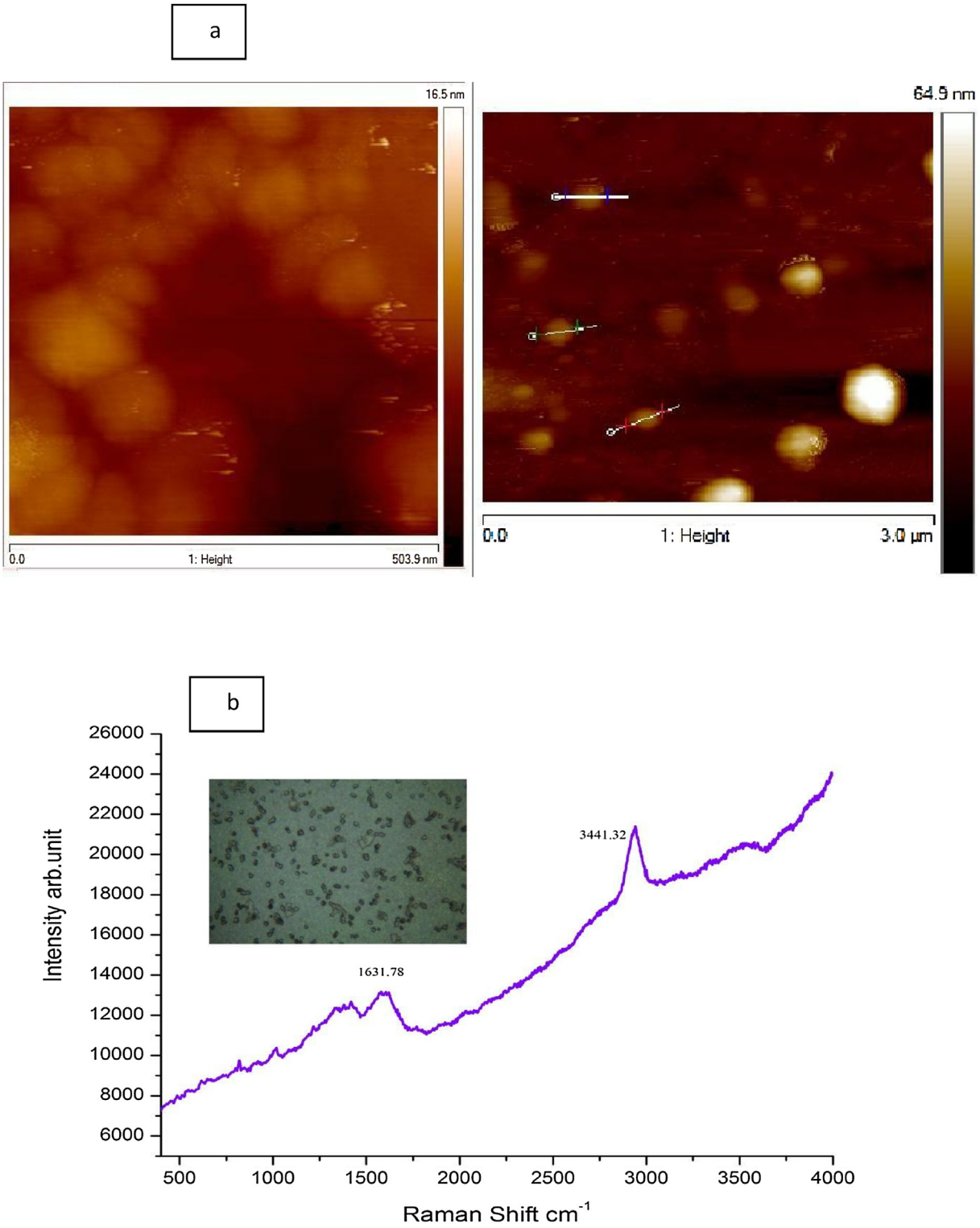

Fig. 3. a AFM revealed the morphology and height of the EPS stabilized AgNPs b. Raman confocal image with the corresponding peaks indicating the presence of Silver and hydroxyl group in EPS-AgNPs.

spectroscopy. A 3 mL of 10^{-5} M aqueous solutions of MO and CR in a quartz cuvette were taken and 5 mg of EPS-AgNPs solution was added separately. To this reaction mixture, 50 mL of 0.1 M $NaBH_4$ was added, and the decreasing absorption maximums of the azo-dyes were recorded [22].

2.7. Statistical analysis

All the experiments were carried out in triplicates and the results were represented as mean ± SD. Data were assessed by analysis of variance and significant differences were found, the

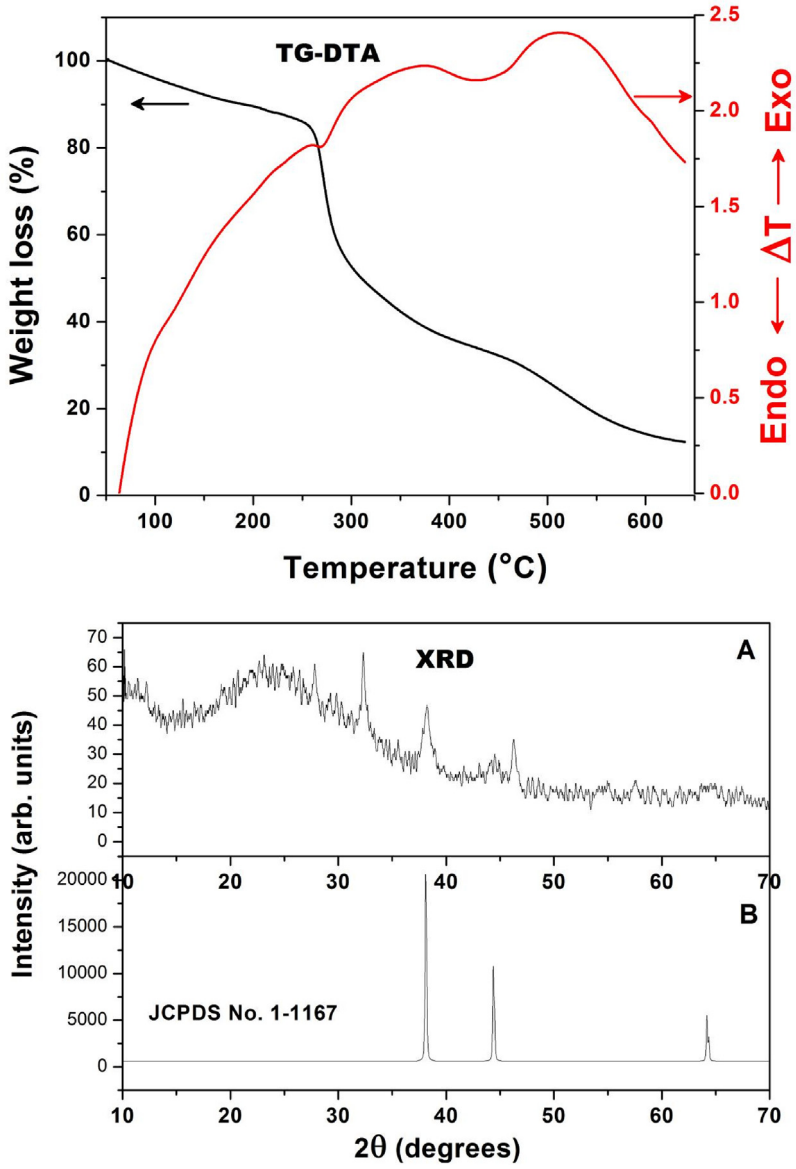

Fig. 4. Thermogravimetic analysis of EPS-AgNPs, XRD-A showed the sample results compare with B standard (JCPDS No.1-1167).

mean was separated by Duncan's multiple range tests with a probability of $p \leq 0.05$ [23]. This analysis was done using SPSS 18.0 for Windows (2007) computer software.

3. Results and discussion

3.1. Characterization of silver nanoparticles

3.1.1. UV–Vis Spectroscopy

EPS-AgNPs (exopolysaccharide-stabilized AgNPs) were synthesized through reduction of Ag^+ into Ag^o from $AgNO_3$.The colourless solution changed to dark yellowish brown colour, indicating the formation of AgNPs, which was monitored in UV–Vis spectra ranges (300–800 nm). The synthesis of polymeric AgNPs after 1, 5, 20 and 30 days of incubation formed a broad surface plasmon resonance absorption band in between 400–550 nm. The intensity of band was increased by increasing storage period up to 1 month in a dark room, indicating the synthesis of AgNPs was increased during the storage period (Fig. 1). Earlier reports [17] showed a strong surface plasmon resonance band at 400–550 nm, indicating the formation of AgNPs. Similar results were observed in *Tribulus terrestris* leaf extract and with polymeric nanoparticles synthesized from *Bacillus subtilis* MSBN17 at the wavelength of 400–450 [24,25]. UV-Visible absorption spectra revealed an absorption maximum wavelength at 425 nm for AgNPs [26].

3.1.2. Transmission electron microscopy (TEM)

TEM is a valuable tool to analyze the size and morphology of nanoparticles. TEM images of EPS-AgNPs (Fig. 2) showed distributed spherical shaped particles with an average size of 35 nm with numerous sizes ranging from 30 to 200 nm [27]. In previous studies, TEM images revealed a size of 30–60 nm spherical-shaped polymeric nanoparticles produced from Cs-Hk fungal cultures, *Streptomyces sp.* MBRC-91and *Bacillus subtilis* MSBN17 [25,28,29]. AgNPs with a size of around 30–50 nm have been reported for bactericidal activity against various pathogens [30,31]. Polymeric nanoparticles ranging from 20 to 200 nm have the maximum potential for *in-vivo* applications [9].

3.1.3. Scanning electron microscopy (SEM)

SEM was used to study the topology of nanoparticles and the process of synthesis from EPS. The EPS-AgNPs synthesis from the

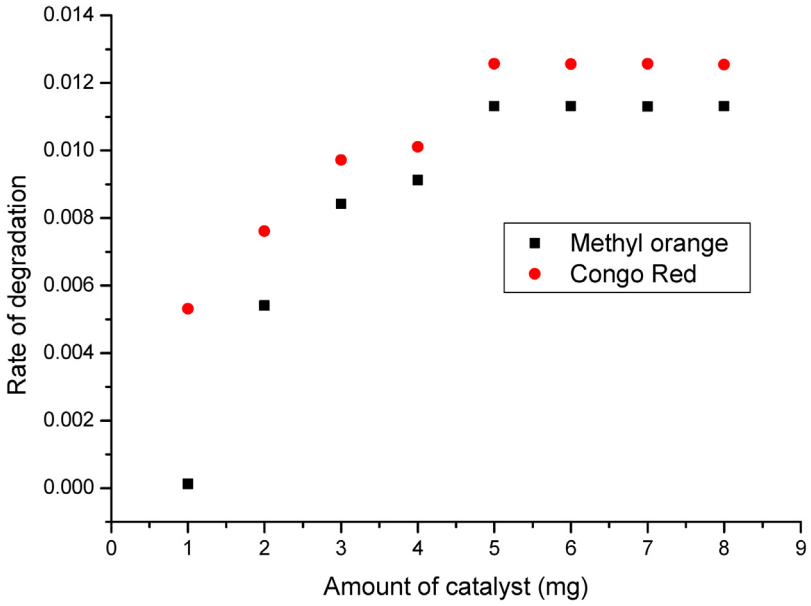

Fig. 5. Catalytic dosage effect of EPS-AgNPs on degradation rate of MO and CR dyes.

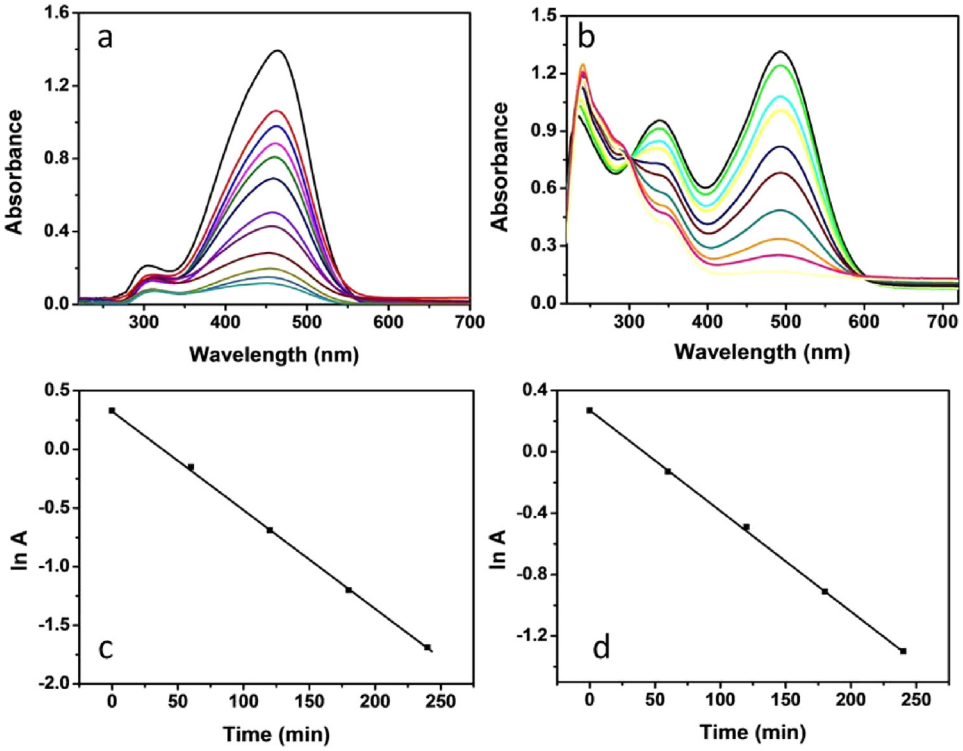

Fig. 6. UV–visible absorption spectra exhibited the degradation of methyl orange (MO) and Congo red (CR) by EPS-AgNPs in the presence of $NaBH_4$. Fig. 6 a and 6 b shows the catalytic degradation of MO and CR respectively with time whereas c and d shows the corresponding ln A versus time plots.

biofilm was observed at 10,000X (Fig. 2). SEM images revealed the presence of spherical shaped EPS-AgNPs at 30,000X, and the dispersion of particles was visualized at 10,000X. Similarly, size, shape and distribution of the SiO_2 nanoparticles were observed through high-resolution SEM [32].

3.1.4. Atomic force microscopy (AFM)

AFM probe analysis was considered in the recent years for the measurement of nanoparticles [33]. The height of the EPS-AgNPs measured at different locations showed an average of 30 nm as similar to TEM image excluding few accumulations (Fig. 3a).

3.1.5. Raman spectroscopy

The EPS-AgNPs image captured in con-focal scanning Raman spectroscopy detected two different peaks. The weak absorption peak exists at 1631.78 cm^{-1}indicating the presence of Ag-C and absorption peak at 3441.32 cm^{-1}, which is associated with stretching vibrations of O-H bond in polymeric nanoparticles

(Fig. 3b) [34]. The FT-IR results of the EPS was published earlier [15].

3.1.6. XRD and TGA-DTA analysis

In EPS-AgNPs, two diffraction peaks at 38.3°and 46.2° with d-spacing 2.76 and 1.9 Å conforming to 111 and 200, planes of crystal structure of metallic silver, was observed in XRD (Fig. 4). These values are described in the literature for silver (JCPDS No.1-1167) [35]. The exothermic peak at 272.13 °C and the required energy is 58.86 J/g with 27.78% weight loss due to the presence of more carboxyl groups in EPS (Fig. 4). Subsequently, another exothermic peak exhibited at 437.1 °C and the required energy is 808.2 J/g with approximately 20% weight loss due to the formation of EPS-AgNPs in TGA-DTA analysis [20].

3.2. Degradation of organic azo-dyes molecules using polymeric AgNPs

To examine the catalytic efficiency of EPS-stabilized AgNPs towards degradation of various organic dye molecules using $NaBH_4$ as a reducing agent, two commercial colors (Methyl orange (MO) and Congo red (CR), commonly used in many dyeing industries have been selected. The degradation reaction was carried out at room temperature and monitored using UV–Visible spectrometry. The catalytic degradation of these dyes was monitored by the change in absorbance at 465 and 495 nm, and then the pseudo-first-order rate constants have been calculated. Degradation of both the dyes was not found to proceed in the absence of either $NaBH_4$ or EPS-AgNPs catalysts. The amount of EPS-AgNPs was varied keeping other parameters as constant to determine the effect of the amount of catalyst on the rate of the degradation. Experiments were performed by using 1 mg to 8 mg of EPS-AgNPs nanomaterial and the results were shown in terms of dye degradation. The degradation rate values were plotted against the amount of catalyst, as shown in Fig. 5. It can be observed, that the rate of degradation increases with the amount of catalyst added upto 5 mg, and further increase in the amount of catalyst did not contribute for the significant enhancement in the degradation rate. Hence, 5 mg of the nanocatalysts has been chosen as the optimum dosage for efficient catalytic degradation of MO and CR dyes. Fig. 6a and 6b shows the catalytic degradation of MO and CR respectively with time, and it can be observed that complete degradation is achieved in 240 minutes with EPS-AgNPs. Fig. 6c and 6d shows the corresponding time versus ln A (linear for a 1st order reaction) plots for the same, and the rate constants were calculated to be $11.31 \times 10^{-3}\,min^{-1}$ and $12.57 \times 10^{-3}\,min^{-1}$ for degradation of MO and CR in the presence of EPS-AgNPs. The catalytic efficiency of the AgNPs stabilized with EPS was found to be playing an important role in degradation of both the dyes. The degradation constants calculated for the prepared EPS-AgNPs towards degradation of MO and CR were found to be better when compared to *Trigonella foenum-graecum* seeds-stabilized AgNPs [36]. Similarly, the degradation of azo dyes by EPS-AgNPs was more effective than the bacterial degradation by the microorganisms such as *Lactobacillus acidophilus, Lactobacillus fermentum* and *Halomonas spp.* [28,37].

The enhanced degradation observed with our nanocatalysts can be attributed to the following reasons: (i) high surface area of the EPS can adsorb azo-dyes; (ii) $NaBH_4$ is expected to act as hydride source, and the AgNPs catalysts are expected to activate the azo nitrogen bond and also to bind with the sulphur and oxygen atoms of the dyes resulting in weakening of azo double bond via conjugation; (iii) large number of oxygen atoms of the EPS could assist in increasing the number of AgNPs; and (iv) EPS networks containing more of hetero atoms are expected to exhibit hydrophilic interactions with azo-dyes, which helps in bringing the dye molecules near the catalytic sites.

4. Conclusion

The green synthesis of AgNPs was performed using bacterial EPS as both, a reducing and stabilizing agent. TEM and SEM analysis revealed that spherical-shaped AgNPs stabilized by EPS thin biofilm have a mean diameter of 35 nm. UV–vis spectroscopy and XRD spectrum revealed the confirmation of EPS-stabilized AgNPs. An excellent thermal property of AgNPs was shown up to 437.1 °C and it can be used to treat textile effluent at higher temperature. The efficient degradation of textile dyes, Methyl orange (MO) and Congo red (CR) was attempted with EPS stabilized AgNPs and it was found to be better than bacterial degradation and AgNPs. These EPS-stabilized AgNPs can be used as environmental friendly and a low cost strategy for degradation of harmful dyes with potential applications in textile industries.

Acknowledgement

The authors are grateful to the Pondicherry University for providing Sophisticated Analytical Instrumental Facility. First author would like to thank DST-PURSE programme for the Ph.D. fellowship.

Appendix A. Supplementary data

Supplementary data associated with this article can be found, in the online version, at http://dx.doi.org/10.1016/j.btre.2017.02.006.

References

[1] P. Sanguansri, M.A. Augustin, Nanoscale materials development-food industry perspective, Trends Food Sci. Tech. 17 (2006) 547–556.
[2] W.T. Liu, Nanoparticles and their biological and environmental applications, J. Biosci.Bioeng. 102 (2006) 1–7.
[3] C. Beer, R. Foldbjerg, Y. Hayashi, D.S. Sutherland, H. Autrup, Toxicity of silver Nanoparticles-Nanoparticle or silver ion? Toxicol.Lett. 208 (2012) 286–292.
[4] I.J. Joye, D.J. McClements, Biopolymer-based nanoparticles and microparticles: Fabrication, characterization, and application, Curr.Opin. Colloid Interf. Sci. 19 (2014) 417–427.
[5] K.B. Narayanan, N. Sakthivel, Biological synthesis of metal nanoparticles by microbes, Adv. Colloid Interfac. 156 (2010) 1–13.
[6] C. Delbarre-Ladrat, C. Sinquin, L. Lebellenger, A. Zykwinska, S. Colliec-Jouault, Exopolysaccharides produced by marine bacteria and their applications as glycosaminoglycan-like molecules, Front. Chem. 2 (2014) 1–15.
[7] M.M. Kemp, A. Kumar, S. Mousa, T.J. Park, P. Ajayan, N. Kubotera, S.A. Mousa, R.J. Linhardt, Synthesis of gold and silver nanoparticles stabilized with glycosaminoglycans having distinctive biological activities, Biomacromol. 10 (2009) 589–595.
[8] Y. Park, Y.N. Hong, A. Weyers, Y.S. Kim, R.J. Linhardt, Polysaccharides and phytochemicals: a natural reservoir for the green synthesis of gold and silver nanoparticles, Nanobiotechnol. IET. 5 (2011) 69–78.
[9] M. Elsabahy, K.L. Wooley, Design of polymeric nanoparticles for biomedical delivery applications, Chem. Soc. Rev. 41 (2012) 2545–2561.
[10] N. Cioffi, M. Rai, Nano-antimicrobials: progress and prospects, First Ed, Springer Science & Business Media, London, 2012.
[11] S.F. Kang, C.H. Liao, S.T. Po, Decolorization of textile wastewater by Photo-Fenton oxidation technology, Chemosphere 41 (2000) 1287–1294.
[12] J. Santhanalakshmi, V. Dhanalakshmi, Chitosan Silver Nanoparticles Assisted Oxidation of Textile Dyes with H_2O_2 Aqueous Solution: Kinetic Studies with pH and Mass Effect, Indian J. Sci. Tech. 5 (2012) 3834–3838.
[13] Y.H. Kim, R. Hensley, Effective control of chlorination and dechlorination at wastewater treatment plants using redox potential, Water Environ. Res. 69 (1997) 1008–1014.
[14] P. Kumar, M. Govindaraju, S. Senthamilselvi, K. Premkumar, Photocatalytic degradation of methyl orange dye using silver (Ag) nanoparticles synthesized from Ulva lactuca, Colloid Surfaces B103 (2013) 658–661.
[15] C. Saravanan, P.K.H. Shetty, Isolation and characterization of exopolysaccharide from *Leuconostoc lactis* KC117496 isolated from idli batter, Int. J. Biol.Macromol. 90 (2016) 100–106.
[16] D. Kavitake, P.B. Devi, S.P. Singh, P.H. Shetty, Characterization of a novel galactan produced by *Weissella confusa* KR780676 from an acidic fermented food, Int. J. Biol.Macromol. 86 (2016) 681–689.

[17] P. Kanmani, S.T. Lim, Synthesis and structural characterization of silver nanoparticles using bacterial exopolysaccharide and its antimicrobial activity against food and multidrug resistant pathogens, Process Biochem. 48 (2013) 1099–1106.
[18] M.K. Shukla, R.P. Singh, C.R.K. Reddy, B. Jha, Synthesis and characterization of agar-based silver nanoparticles and nanocomposite film with antibacterial applications, Bioresour. Technol. 107 (2012) 295–300.
[19] Z. Ahmed, Y. Wang, N. Anjum, A. Ahmad, S.T. Khan, Characterization of exopolysaccharide produced by *Lactobacillus kefiranofaciens* ZW3 isolated from Tibet kefir Part II, Food Hydrocoll. 30 (2013) 343–350.
[20] Y. Wang, C. Li, P. Liu, Z. Ahmed, P. Xiao, X. Bai, Physical characterization of exopolysaccharide produced by *Lactobacillus plantarum* KF5 isolated from Tibet Kefir, Carbohyd.Polym. 82 (2010) 895–903.
[21] K.R. Kumar, Third order nonlinear optical properties of bismuth zinc borate glasses, J. Appl. Phys. 114 (2013) 1–6 243103.
[22] R. Rajesh, E. Sujanthi, S.S. Kumar, R. Venkatesan, Designing versatile heterogeneous catalysts based on Ag and Au nanoparticles decorated on chitosan functionalized graphene oxide, Phys. Chem. Chem. Phys. 17 (2015) 11329–11340.
[23] D.B. Duncan, Multiple range and multiple F tests, Biometrics 11 (1955) 1–42.
[24] S. Ashokkumar, S. Ravi, V. Kathiravan, S. Velmurugan, SpectrochimActa, Synthesis. characterization and catalytic activity of silver nanoparticles using Tribulusterrestris leaf extract 121 (2014) 88–93.
[25] G. Sathiyanarayanan, G.S. Kiran, J. Selvin, Synthesis of silver nanoparticles by polysaccharide bioflocculant produced from marine Bacillus subtilis MSBN17, Colloid Surface B102 (2013) 13–20.
[26] S.S. Khan, A. Mukherjee, N. Chandrasekaran, Interaction of colloidal silver nanoparticles (SNPs) with exopolysaccharides (EPS) and its adsorption isotherms and kinetics, Colloid Surface A381 (2011) 99–105.
[27] A.C. Raveendran, Y. Poulose, T. Yoshida, Bacterial exopolysaccharide based nanoparticles for sustained drug delivery, cancer chemotherapy and bioimaging, Carbohyd Polym . 91 (2013) 22–32.
[28] X. Chen, J.K. Yan, J.Y. Wu, Characterization and antibacterial activity of silver nanoparticles prepared with a fungal exopolysaccharide in water, Food Hydrocoll 53 (2015) 69–74.
[29] P. Manivasagan, K.H. Kang, D.G. Kim, S.K. Kim, Production of polysaccharide-based bioflocculant for the synthesis of silver nanoparticles by *Streptomyces* sp, Int. J. Biol.Macromol. 77 (2015) 159–167.
[30] F. Kang, P.J. Alvarez, D. Zhu, Microbial extracellular polymeric substances reduce Ag+ to silver nanoparticles and antagonize bactericidal activity, Environ. Sci. Technol 48 (2013) 316–322.
[31] Y. Liu, Z. Zheng, J.N. Zara, C. Hsu, D.E. Soofer, K.S. Lee, R.K. Siu, L.S. Miller, X. Zhang, D. Carpenter, The antimicrobial and osteo inductive properties of silver nanoparticle/poly (DL-lactic-co-glycolic acid)-coated stainless steel, Biomaterials 33 (2012) 8745–8756.
[32] V.D. Hodoroaba, S. Rades, W.E.S. Unger, Inspection of morphology and elemental imaging of single nanoparticles by high resolution SEM/EDX in transmission mode, Surf. Interface Anal. 46 (2014) 945–948.
[33] P. Klapetek, M. Valtr, D. NeAas, O. Salyk, P. Dzik, Atomic force microscopy analysis of nanoparticles in non-ideal conditions, Nanoscale Res. Lett 6 (2011) 1–9.
[34] A.M. Shakourim, N.M. Salavati, Structural and spectroscopic characterization of prepared Ag 2 S nanoparticles with a novel sulfuring agent, Spectrochim Acta A 133 (2014) 463–471.
[35] E.J. Lee, L. Piao, J.K. Kim, Synthesis of silver nanoparticles from the decomposition of silver(I) [bis (alkylthio) methylene] malonate complexes, Bull. Korean Chem. Soc. 33 (2012) 60–64.
[36] V.K. Vidhu, D. Philip, Catalytic degradation of organic dyes using biosynthesized silver nanoparticles, Micron 56 (2014) 54–62.
[37] S. Asad, M.A. Amoozegar, A.A. Pourbabaee, M.N. Sarbolouki, S.M.M. Dastgheib, Decolorization of textile azo dyes by newly isolated halophilic and halotolerant bacteria, Bioresour. Technol 98 (2007) 2082–2088.